JCTC Journal of Chemical Theory and Computation

Article

pubs.acs.org/JCTC

Implementation of Two-Component Time-Dependent Density Functional Theory in TURBOMOLE

Michael Kühn[†] and Florian Weigend*[,†,‡]

[†]Institut für Physikalische Chemie, Karlsruher Institut für Technologie, Kaiserstraße 12, 76131 Karlsruhe, Germany

[‡]Institut für Nanotechnologie, Karlsruher Institut für Technologie, Postfach 3640, 76021 Karlsruhe, Germany

Supporting Information

ABSTRACT: We report the efficient implementation of a two-component time-dependent density functional theory proposed by Wang et al. (Wang, F.; Ziegler, T.; van Lenthe, E.; van Gisbergen, S.; Baerends, E. J. *J. Chem. Phys.* **2005**, *122*, 204103) that accounts for spin−orbit effects on excitations of closed-shell systems by employing a noncollinear exchange−correlation kernel. In contrast to the aforementioned implementation, our method is based on two-component effective core potentials as well as Gaussian-type basis functions. It is implemented in the TURBOMOLE program suite for functionals of the local density approximation and the generalized gradient approximation. Accuracy is assessed by comparison of two-component vertical excitation energies of heavy atoms and ions (Cd, Hg, Au^+) and small molecules (I_2, TlH) to other two- and four-component approaches. Efficiency is demonstrated by calculating the electronic spectrum of Au_{20}.

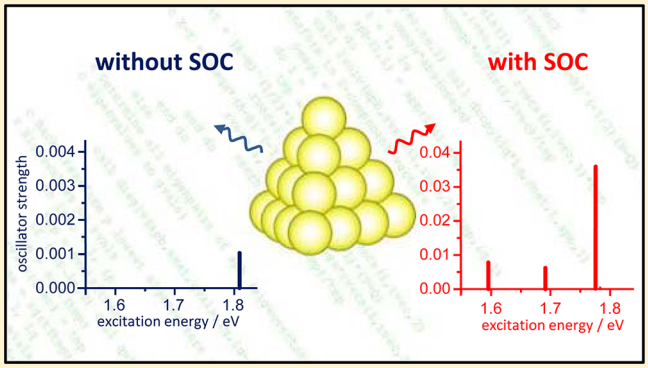

1. INTRODUCTION

Time-dependent density functional theory (TDDFT)[2,3] is widely used for the calculation of electronic excitations of large systems. Especially for systems containing heavy elements, relativistic effects on spectra become important and need to be incorporated. For most quantum−chemical programs this is limited to scalar relativistic effects. Their incorporation does not change the program structure; like in nonrelativistic treatments, one-component real molecular orbitals (MOs) can be used. Matrix elements describing these scalar relativistic effects usually are either obtained via zeroth-order regular approximation (ZORA)[4−7] or modeled by one-component scalar relativistic (1c) effective core potentials (ECPs), e.g., Wood-Boring ECPs, that are available for elements beyond Kr (4d and 5d,[8] group 13−18,[9,10] group 1,[11] and group 2[12]). However, in 1c TDDFT, the effect of spin−orbit coupling (SOC) is neglected, and therefore, this variant of relativistic TDDFT is not able to calculate intensities of so-called "spin-forbidden" transitions, in particular phosphorescence.

When going beyond, the most fundamental way is fully relativistic TDDFT using four-component (4c) complex spinors[13] based on the Dirac−Coulomb Hamiltonian.[14−16] A more economic alternative of very similar accuracy for chemistry is quasi-relativistic TDDFT using two-component (2c) complex spinors,[1,17] where the small component is removed. This reduces the size of the problem and requires smaller basis sets than the 4c treatment. Moreover, it is easier to implement this variant in an existing 1c TDDFT code.

Presently available are 2c TDDFT implementations by Wang, Ziegler, van Lenthe, van Gisbergen, and Baerends[1] in the Amsterdam density functional program package (ADF)[18] and by Peng, Zou, and Liu[17] in the Beijing density functional program package (BDF)[19−21] employing the ZORA model[5−7] for the relativistic Hamiltonian. Furthermore, Bast, Jensen, and Saue[16] claim that their 4c adiabatic TDDFT implementation in the Dirac program package[22] based on the Dirac−Coulomb Hamiltonian is operational for the exact 2c Hamiltonian (X2C).[23] All these implementations work for Kramers-restricted closed-shell systems and exchange−correlation (XC) functionals of the local density approximation (LDA). Additionally, the 4c implementation by Bast et al. includes hybrid generalized gradient approximation (GGA) functionals using proper XC kernels (full derivatives of functionals).[16]

Because there is no response of the relativistic operators used in the work of Wang et al.[1] and Peng et al.[17] to an external time-dependent perturbation within adiabatic TDDFT, at first sight it seems that it is sufficient to just implement a 2c version of an already existing 1c code, as all relativistic effects on spectra arise from the corresponding ground-state spinors and their energies only. However, because isotropy in moment (spin) space of the XC kernel is required for obtaining the correct nonrelativistic limit for both 4c and 2c TDDFT, a noncollinear formulation has to be utilized.[24,25] There are no relativistic corrections to the (adiabatic) XC kernel as experience has

Received: August 21, 2013
Published: November 5, 2013

shown that they have only small effects on valence properties of heavy elements.[26−28]

Whereas at the 1c level, systems with several 100 atoms (several thousand basis functions) may routinely be calculated (on a single processor), for 2c treatments systems reported are of rather moderate size. To the best of our knowledge, the largest systems calculated so far using the efficient 2c ADF TDDFT implementation are the few lowest (up to several ten) excited states (including spatial degeneracies) of $[PtBr_4]^{2-}$,[29] [Au(diethynyl-(9-(dicyanomethylene)fluorene))],[30] [Re(CO)$_3$(1,10-phenanthroline)Cl],[31] $[Mo_6I_8I_6]^{2-}$,[32] $[Au_3(CH_3N{=}COCH_3)_3]$,[33] $[Au_2$(hexaphyrin)],[34] and [Ir(8-hydroxyquinolate)$_3$],[35] using polarized triple-ζ basis sets. There are also calculations on [Ir(2-phenylpyridine)(2-(2,4-difluorophenyl)pyridine)(acetylacetonate)],[36] [Ir(2-(2,4-dibromophenylpyridine))$_2$(picolinate)],[37] and [ReI(CO)$_3$(2,2′-bipyridine)][38] employing polarized triple-ζ basis sets for the metal atom and polarized double-ζ basis sets for all other atoms. Calculations on systems using polarized quadruple-ζ basis sets are either restricted to smaller systems like [Ti(η^5-C_5H_5)$_2$Cl$_2$][39] or very few excited states. The largest system calculated so far is $[TaAu_{12}]^-$.[40] However, only polarized triple-ζ basis sets have been employed, while core electrons have been kept frozen up to 4f for both elements. The largest system calculated so far using the 4c TDDFT implementation of Bast et al.[16] that is also able to employ a proper 2c XC GGA kernel based on the X2C method is $[UO_2Cl_4]^{2-}$ (basis sets of triple-ζ quality, lowest 15 excited states).[41]

Our goal is to provide a 2c TDDFT implementation that allows for routine treatments of systems with several thousand basis functions on a single processor as well as reasonable scaling for moderately parallelized tasks. This is done by following the formalism derived by Wang et al.[1] and Peng et al.[17] but using 2c ECPs instead of the ZORA methodology and Gaussian- instead of Slater-type basis functions. 2c ECPs have already been successfully used to describe the effect of SOC on ground-state properties of systems containing heavy elements within density functional theory (DFT) using an efficient 2c implementation in the TURBOMOLE program package.[42,43] 2c Dirac−Hartree−Fock ECPs (dhf-ECPs) are available for elements beyond Kr (4d,[44] 5d,[45] group 11−12,[46] group 13−15,[47] group 16−18,[48] group 1,[49] and group 2[50]). As a result of using ECPs instead of the all-electron ZORA methodology, only valence electrons have to be treated explicitly in the TDDFT calculation. This leads to significant savings in computation time. Within the ECP formalism, SOC matrix elements result only for heavy atoms where ECPs are employed, whereas within the ZORA formalism, there are SOC matrix elements for each atom. The above-mentioned ECPs are fitted to 4c multiconfiguration Dirac−Hartree−Fock calculations on atoms and contain exchange, correlation, and relativistic contributions. Therefore, relativistic effects (also two-electron relativistic interactions) are included to higher order than in ZORA, however, unsystematically. Furthermore, by using TURBOMOLE as the platform for the implementation, we benefit from efficient integral routines using Gaussian-type basis functions. It is a common belief that concerning efficiency this type of functions is superior to Slater-type basis functions used by Wang et al.,[1] which may have other merits.

The paper is organized as follows. In Section 2, we briefly summarize the theory of 2c TDDFT for Kramers-restricted closed-shell cases and give some details specific to our implementation. In Section 3, we assess the accuracy of our implementation by comparing the excitation energies of the $s\rightarrow p$ transitions in Cd and Hg to the 2c variant given in ref 1 as well as to two different 4c approaches[15,16] and experimental results. The excitation energies of the $d\rightarrow s$ transitions in Au^+ and of the lowest transitions in I_2 and TlH are compared to the results obtained in ref 1 and experimental studies. We further demonstrate the efficiency of our implementation calculating the lowest 57 excitations of tedrahedral Au_{20} using quadruple-ζ basis sets. This is the first TDDFT calculation on Au_{20} including SOC, which is demonstrated to have a non-negligible effect on the electronic spectrum.

2. TWO-COMPONENT TIME-DEPENDENT DENSITY FUNCTIONAL THEORY

Wang et al.[1] as well as Peng et al.[17] proposed a 2c TDDFT that accounts for SOC effects on excitations of systems possessing a Kramers-restricted closed-shell ground state (time-reversal symmetry exploited) by employing a noncollinear XC potential.

The approximate time-dependent Kohn−Sham (TDKS) eigenvalue problem for excitation energies ω using pure density functionals is very similar to that of 1c TDDFT

$$\Omega_{i\tilde{\sigma}a\tilde{\tau}j\tilde{\sigma}'b\tilde{\tau}'}(X+Y)'_{j\tilde{\sigma}'b\tilde{\tau}'} = \omega^2(X+Y)'_{i\tilde{\sigma}a\tilde{\tau}} \tag{1}$$

with

$$\Omega_{i\tilde{\sigma}a\tilde{\tau}j\tilde{\sigma}'b\tilde{\tau}'} = (\varepsilon_{a\tilde{\tau}} - \varepsilon_{i\tilde{\sigma}})^2\delta_{ij}\delta_{ab}\delta_{\tilde{\sigma}\tilde{\sigma}}\delta_{\tilde{\tau}\tilde{\tau}'} + 2\sqrt{\varepsilon_{a\tilde{\tau}} - \varepsilon_{i\tilde{\sigma}}} \times C_{i\tilde{\sigma}a\tilde{\tau}j\tilde{\sigma}'b\tilde{\tau}'}\sqrt{\varepsilon_{b\tilde{\tau}'} - \varepsilon_{j\tilde{\sigma}'}} \tag{2}$$

where indices i, j, ... are used for occupied, a, b, ... for virtual and p, q, ... for general molecular spinors. Greek indices $\tilde{\sigma}$, $\tilde{\tau}$, $\tilde{\sigma}'$, and $\tilde{\tau}' \in \{\tilde{\alpha}, \tilde{\beta}\}$ refer to 2c time-reversal symmetry-adapted Kramers partners describing $N_{\tilde{\alpha}}$ moment-up ($\tilde{\alpha}$) and $N_{\tilde{\beta}}$ moment-down ($\tilde{\beta}$) electrons. For a Kramers-restricted closed-shell system is $N_{\tilde{\alpha}} = N_{\tilde{\beta}} = (1/2)N$. The total number of orbitals (occupied plus virtual) is $M_{\tilde{\alpha}} = N_{\tilde{\alpha}} + N_{\tilde{\alpha}}^{\mathrm{virt}}$ and $M_{\tilde{\beta}} = N_{\tilde{\beta}} + N_{\tilde{\beta}}^{\mathrm{virt}}$, respectively. $\varepsilon_{p\tilde{\sigma}}$ describes the energy of spinor p with Kramers index $\tilde{\sigma}$ and δ_{pq} is the Kronecker delta. Note that eq 1 is approximate in the sense that the transformation yielding this equation is not exact if SOC is present. However, Wang et al. claim that test calculations show errors always less than 0.05 eV.[1] Peng et al. state that this approximation may not work if either the excitation energy is not close to the orbital energy difference or if there are highly inhomogeneous induced fields (e.g., localized nonfully filled f spinors of a formally closed-shell system).[17]

The resulting expression for the complex (Hermitian) coupling matrix $C_{i\tilde{\sigma}a\tilde{\tau}j\tilde{\sigma}'b\tilde{\tau}'}$ reads

$$C_{i\tilde{\sigma}a\tilde{\tau}j\tilde{\sigma}'b\tilde{\tau}'} = \langle\Phi_{i\tilde{\sigma}}\Phi_{b\tilde{\tau}'}|\Phi_{a\tilde{\tau}}\Phi_{j\tilde{\sigma}'}\rangle + \langle\Phi_{i\tilde{\sigma}}\Phi_{b\tilde{\tau}'}|\mathbf{f}_{\mathrm{XC}}|\Phi_{a\tilde{\tau}}\Phi_{j\tilde{\sigma}'}\rangle \tag{3}$$

The first term is the Coulomb matrix element in Dirac notation. The second term is the matrix element of the noncollinear XC kernel. Because both the 2c ZORA kinetic operator and the 2c ECP are one-electron operators that account for SOC, they do not respond to a TD external perturbation. As a result there is no additional SOC contribution to $C_{i\tilde{\sigma}a\tilde{\tau}j\tilde{\sigma}'b\tilde{\tau}'}$, and SOC effects on spectra arise via the ground-state spinors and their energies only. $\Phi_{p\tilde{\sigma}}$ are complex 2c spinors that are not necessarily eigenfunctions of $\hat{\mathbf{S}}_z = (1/2)\sigma_z$.

The noncollinear XC kernel within the adiabatic approximation is

$$\mathbf{f}_{XC}(\vec{r},\vec{r}') = \frac{\delta^2 E_{XC}}{\delta\rho(\vec{r})\delta\rho(\vec{r}')}\mathbf{1}\otimes\mathbf{1} + \sum_{k=x,y,z}\frac{\delta^2 E_{XC}}{\delta s^2(\vec{r})} \times \delta(\vec{r}-\vec{r}')\sigma_k\otimes\sigma_k \quad (4)$$

$s(\vec{r}) = |\vec{m}(\vec{r})|$ is the noncollinear spin density with the magnetization vector $\vec{m}(\vec{r}) = \sum_{\tilde{\sigma}}\sum_{i=1}^{N_{\tilde{\sigma}}}\Phi^{\dagger}_{i\tilde{\sigma}}(\vec{r})\vec{\sigma}\Phi_{i\tilde{\sigma}}(\vec{r})$. The total density is defined as $\rho(\vec{r}) = \sum_{\tilde{\sigma}}\sum_{i=1}^{N_{\tilde{\sigma}}}\Phi^{\dagger}_{i\tilde{\sigma}}(\vec{r})\Phi_{i\tilde{\sigma}}(\vec{r})$ and E_{XC} is the nonrelativistic XC energy depending on ρ and s. The left side of the tensor product refers to indices i and a, whereas the right side refers to j and b.

The noncollinear XC kernel, if considered in AO basis, can be divided into two nonmixing parts: one is closely related to the 1c collinear XC kernel for singlet−singlet transitions and the other one to that for singlet−triplet transitions.[51] Therefore, the noncollinear GGA XC kernel can be derived from the 1c collinear GGA XC kernels for singlet−singlet and singlet−triplet transitions in an analogous manner as the noncollinear LDA XC kernel (essentially eq 4) from the 1c collinear LDA XC kernels.

We note in passing that the noncollinear GGA XC kernel used in spin-flip TDDFT[52,53] (variant of open-shell TDDFT that is able to describe transitions, for which the z component of the total spin of the system changes by ±1, $\Delta S_z = \pm 1$) is known to possess singularities at points where the collinear spin density but not the gradient of this spin density is zero.[54−57] This problem does not occur in case of the presented 2c TDDFT formalism because the problematic term with the spin density in the denominator, $(1/s(\vec{r}))(\delta E_{XC}/\delta s(\vec{r}))$, becomes $\delta^2 E_{XC}/\delta s^2(\vec{r})$ for (Kramers-restricted) closed-shell systems.

We also note that the extension of 2c TDDFT to hybrid functionals requires solving the general and exact TDKS eigenvalue problem (eq 5 in ref 17). Simplifications for Kramers-restricted closed-shell systems[1,17] leading to eq 1 are not possible if Hartree−Fock exchange is included. This is already the case for 1c TDDFT. Unlike in 1c TDDFT, the extension of 2c TDDFT to open-shell systems also requires solving the general TDKS eigenvalue problem with a quite involved structure of the XC kernel.[17,52]

This 2c TDDFT based on a noncollinear XC potential has the correct nonrelativistic limit and therefore yields both singlet ($\sigma = \tau$ and $\sigma' = \tau'$) and triplet excitations ($\sigma \neq \tau$ and $\sigma' \neq \tau'$), the latter with the correct 3-fold degeneracy. In the nonrelativistic limit, moment-up/moment-down ($\tilde{\alpha}/\tilde{\beta}$) electrons become ordinary spin-up/spin-down (α/β) electrons. As a result the coupling matrix $C_{i\sigma a\tau j\sigma' b\tau'}$ is real, the MOs $\Phi_{p\sigma}$ are eigenfunctions of $\hat{\mathbf{S}}_z$, and the XC kernel can be chosen to be collinear in this case.

2c TDDFT is more demanding concerning computation time and required memory than 1c TDDFT. For 1c closed-shell TDDFT that describes both singlet and triplet excitations (the latter without the correct degeneracy), the dimension of $(X+Y)'_{i\sigma a\tau}$ is dim = $\sum_{\sigma\tau}N_\sigma \times N^{\mathrm{virt}}_\tau\delta_{\sigma\tau} = (1/2)N \times N^{\mathrm{virt}}$. Such a 1c closed-shell TDDFT is identical to a 1c open-shell spin-preserving (z-component of the total spin of the system remains unchanged) TDDFT that is applied to a formally closed-shell ground state. In 2c Kramers-restricted closed-shell TDDFT, the dimension of $(X+Y)'_{i\tilde{\sigma}a\tilde{\tau}}$ is dim = $\sum_{\tilde{\sigma}\tilde{\tau}}N_{\tilde{\sigma}} \times N^{\mathrm{virt}}_{\tilde{\tau}} = 2N \times N^{\mathrm{virt}}$, which is 4 times larger (the factor of 2 arises because the excitation vectors $(X+Y)'_{i\tilde{\sigma}a\tilde{\tau}}$ are complex). In the basis of atomic orbitals (AOs), the excitation vectors are also 4 times larger within the 2c formalism.

Using the converged $(X+Y)'_{i\tilde{\sigma}a\tilde{\tau},n}$ and ω_n, the linear response of the dipole operator $\delta\langle\vec{\mu}\rangle_n$ that corresponds to the electric transition dipole moment $\langle 0|\vec{\mu}|n\rangle$ for the transition from the ground state to an excited state n reads (e.g., in length representation)

$$\langle 0|\vec{\mu}|n\rangle = \delta\langle\vec{\mu}\rangle_n = \sum_{\tilde{\sigma}\tilde{\tau}}\sum_{i=1}^{N_{\tilde{\sigma}}}\sum_{a=N_{\tilde{\tau}}+1}^{M_{\tilde{\tau}}}\frac{1}{\sqrt{\omega_n}}\sqrt{\varepsilon_{a\tilde{\tau}}-\varepsilon_{i\tilde{\sigma}}}(X+Y)'_{i\tilde{\sigma}a\tilde{\tau},n} \times \langle\Phi_{a\tilde{\tau}}|\vec{\mu}\,\mathbf{1}|\Phi_{i\tilde{\sigma}}\rangle \quad (5)$$

Oscillator strengths (OSs) are then calculated using the expression

$$f_{0n} = \frac{2}{3}\omega_n|\langle 0|\vec{\mu}|n\rangle|^2 \quad (6)$$

Equations 1−6 were implemented in the ESCF excited-state module[51,55,58,59] of the TURBOMOLE program suite, mainly by extending the already existing 1c routines to the 2c formalism. In particular, a 2c noncollinear XC kernel for closed-shell systems had to be implemented as well as a complex diagonalizing Davidson algorithm[60,61] to solve eq 1. Details of the implemented procedure are given in Figure I of the Supporting Information. Striving for high efficiency, our implementation is based on 2c ECPs as well as Gaussian-type basis functions instead of ZORA and Slater-type basis functions used in the ADF implementation. Our code utilizes the resolution of the identity (RI) approximation[59,62] and is also parallelized employing the technique by van Wüllen[63] in the same way as for the 1c case. Our implementation works for LDA as well as GGA functionals. To the best of our knowledge, this is the first implementation of a proper GGA XC kernel in an efficient 2c TDDFT algorithm using full derivatives of functionals. The conductor-like screening model (COSMO)[64,65] that considers solvent effects is also implemented in our 2c TDDFT code.

3. APPLICATIONS

Computational Details. All ground-state closed-shell structures of diatomic molecules were optimized using 1c DFT and the GGA functional of Becke and Perdew (BP86)[66,67] in combination with polarized quadruple-ζ valence basis sets (dhf-QZVP-2c).[68] The dhf-bases are optimized for the usage in connection with Dirac−Hartree−Fock ECPs (dhf-ECPs), which account for scalar relativistic effects in 1c calculations and additionally for SOC effects in 2c calculations. For Cd and I, pseudopotentials (dhf-ECP-28)[46,48] covering the inner 28 electrons were used; for Au, Hg, and Tl, pseudopotentials (dhf-ECP-60)[46,47] covering the inner 60 electrons were used. The ground-state closed-shell structure of Au_{20} was optimized assuming T_d symmetry and using 1c DFT with the meta-GGA functional of Tao, Perdew, Staroverov, and Scuseria (TPSS)[69] in combination with a doubly polarized quadruple-ζ valence basis sets (dhf-QZVPP-2c).[68] Coordinates of all optimized structures are available in Tables VII−IX of the Supporting Information.

Vertical excitation energies (VEEs) were computed at both the 1c and 2c TDDFT level using the Perdew−Wang parametrization of the local spin-density approximation (LSDA)[70] and the GGA functional BP86.[66,67] dhf-QZVPP-2c and dhf-QZVP-2c basis sets as well as basis sets of polarized

Table 1. Two-Component (2c) Vertical Excitation Energies (VEEs) for $s \rightarrow p$ Transitions, Fine-Structure Splittings, and Shifts (given relatively to average of triplet state) of Cd and Hg[a]

atom		g_J	BP86	LSDA	ref 1	ref 15	ref 16	exp.
Cd	average of triplet state		3.804 (3.808)	4.195 (4.199)	4.098	4.12	4.10	3.874
	splitting of $^3P_0$	1	−0.142	−0.141	−0.148	−0.15	−0.15	−0.140
	splitting of $^3P_1$	3	−0.073	−0.074	−0.077	−0.08	−0.08	−0.073
	splitting of $^3P_2$	5	0.072	0.072	0.076	0.07	0.07	0.072
	shift of $^1P_1$	3	1.534 (1.532)	1.271 (1.269)	1.251	1.38	1.24	1.543
Hg	average of triplet state		5.058 (5.114)	5.411 (5.470)	5.387	5.41	5.38	5.181
	splitting of $^3P_0$	1	−0.489	−0.492	−0.516	−0.52	−0.51	−0.514
	splitting of $^3P_1$	3	−0.275	−0.287	−0.301	−0.29	−0.30	−0.295
	splitting of $^3P_2$	5	0.263	0.270	0.284	0.28	0.29	0.280
	shift of $^1P_1$	3	1.388 (1.368)	1.156 (1.131)	1.144	1.25	1.15	1.523

[a]All calculated values were obtained using the the BP86 and LSDA functional in combination with dhf-QZVP-2c basis sets and dhf-ecp-2c spin-orbit effective core potentials (ECPs). Values in parentheses are scalar relativistic (1c) results for ^3P and ^1P states. Degeneracies $g_J = (2J + 1)$ are also given. All values are in eV. 2c VEEs obtained by Wang et al. are listed in column "ref 1", 4c VEEs by Gao et al. in column "ref 15", and those by Bast et al. in column "ref 16". Experimental results are from ref 75 .

triple-ζ quality (dhf-TZVP-2c) were used.[68] Diffuse-augmented dhf-QZVPD-2c bases[71] from the hierarchy of property-optimized basis sets were not investigated because for Cd, Hg, and Au, dhf-QZVPD-2c is identical to dhf-QZVP-2c. OSs were calculated using velocity and length representations. The iterative Davidson procedure in TDDFT calculations is stopped when the Euclidean norm of the residual vector is smaller than 10^{-5} a.u.

In all calculations, the RI approximation[59] is employed with auxiliary basis sets[72] that are suited for bases optimized for dhf-ECPs.[73] Reference state energies and density matrices were converged to 10^{-7} a.u. Fine quadrature grids of size m4[74] were employed.

For Au_{20}, the lowest 10 VEEs and OSs were additionally calculated at the 2c BP86/QZVPP level using more strict convergence criteria and very fine quadrature grids. Reference state energies and density matrices were converged to 10^{-10} a.u. The iterative Davidson procedure in TDDFT calculations is stopped when the Euclidean norm of the residual vector is smaller than 10^{-8} a.u. Quadrature grids of size 5[74] were employed. VEEs systematically deviate about −0.0002 eV, and OSs in the order of 10^{-4} (10^{-10}) have a maximum absolute deviation in the order of 10^{-7} (10^{-11}) from the results obtained using less strict convergence criteria and coarser quadrature grids.

3.1. Assessment of Accuracy: Excitation Energies and Fine-Structure Splittings of Selected Closed-Shell Atoms, Ions, and Diatomic Molecules. We calculated 2c and 1c VEEs using QZVP basis sets in combination with the LSDA and BP86 functional for the $s \rightarrow p$ transitions in Cd and Hg and for the $d \rightarrow s$ transitions in Au^+, as well as for the lowest 12 transitions in I_2 and the lowest 5 transitions in TlH. Comparison of VEEs obtained with the present 2c implementation (ECPs, Gaussian-type basis functions) to data reported by Wang et al.[1] (ZORA, Slater-type basis functions) as well as to 4c treatments[15,16] (in the cases of Cd and Hg) showed small deviations among these methods, usually less than 0.1 eV. These deviations are much smaller than most differences to experimental data.[75,78]

In detail, we start by comparing the VEEs for the $s \rightarrow p$ transitions in atomic Cd and Hg obtained with the present 2c implementation to reported data. Quantities of interest are the average VEE for the triplet excitation (^3P), the respective splittings, and the energy difference to the singlet (^1P) transition ("shift") (Table 1). Reported data were obtained with the LDA-type functional SVWN[79−81] and quadruple-ζ[1] or triple-ζ[15,16] all-electron basis sets. For VEEs concerning the singlet−triplet transitions, the three reported methods and our implementation when employing the LDA-type functional LSDA agree typically within 0.01 eV, the largest difference is observed for the $^3P_0$ state of Hg, 0.028 eV between our implementation and ref 15. Concerning the "shift" of the singlet−singlet ($^1P_1$) transition, results are similar except for ref 15, which differs from the other results by slightly more than 0.1 eV for both Cd and Hg. Comparison to experimental data shows excellent agreement for splittings of the triplet sublevels (error of up to 0.02 eV), but comparably large errors for the average VEE of the triplet state and for the "shift" of the $^1P_1$ excitation (ca. 0.3 eV). This is not specific for the 2c or the 4c variant of TDDFT but for TDDFT itself. The average VEEs for the triplet excitation and the VEE for the singlet transition are accessible also from 1c TDDFT; they deviate from the 2c results by less than about 0.05 eV. The GGA functional BP86 leads to significant improvements in accuracy of average triplet and singlet VEEs. With this, functional errors for Cd are below 0.1 eV and for Hg below 0.15 eV. Results for triplet splittings do not change much.

For the $d \rightarrow s$ transitions in Au^+, again differences in VEEs between the present implementation and that by Wang et al.[1] are very small, 0.07 eV at most (Table 2). Comparison to experimental data shows some problems. The average VEE of the triplet excitation is underestimated by about 0.8 eV, and the splitting of the $^3D_2$ state is calculated to −0.020 eV (our implementation) or −0.028 eV (ref 1), whereas the experimental value is −0.101 eV. For this system, also employing the BP86 functional is not helpful; errors become even slightly larger. 2c treatments show significant differences to 1c treatments here. In the 2c case, the average VEE of the triplet state is about 0.15 eV lower, whereas the singlet VEE is about 0.5 eV higher compared to the 1c case. This is a consequence of the splitting of the fully occupied d orbitals by SOC, which is neglected in 1c treatments. The triplet excitation mainly involves the $d_{5/2}$ level (in the 2c case), the energy of which is slightly higher than that of the d shell in the 1c case; thus the energy difference to the unoccupied 6s, which is the lowest VEE in zeroth order, is smaller for the 2c than for the 1c case. The singlet excitation mainly involves the $d_{3/2}$ level, which is lower in energy than the d shell in the 1c case. This leads to a

Table 2. Two-Component (2c) Vertical Excitation Energies (VEEs) for $d \rightarrow s$ Transitions, Fine-Structure Splittings, and Shifts (given relatively to average of triplet state) of Au^+[a]

	g_J	BP86	LSDA	ref 1	exp.
average of triplet state		1.429 (1.576)	1.498 (1.642)	1.501	2.288
splitting of $^3D_3$	7	−0.506	−0.454	−0.481	−0.423
splitting of $^3D_2$	5	−0.027	−0.020	−0.028	−0.101
splitting of $^3D_1$	3	1.136	1.092	1.168	1.155
shift of $^1D_2$	5	1.663 (1.165)	1.531 (1.002)	1.609	1.385

[a]All calculated values were obtained using the BP86 and LSDA functional in combination with the dhf-QZVP-2c basis set and dhf-ecp-2c spin-orbit effective core potential (ECP). Values in parentheses are scalar relativistic (1c) results for ^3D and ^1D states. Degeneracies $g_J = (2J + 1)$ are also given. All values are in eV. 2c VEEs obtained by Wang et al. are listed in column "ref 15". Experimental results are from ref 75.

larger energy difference to the 6*s* shell and thus to a higher VEE. Employing COSMO (refractive index $n = 1.33$, relative permittivity $\varepsilon_r = 80$) leads to slightly (up to 0.06 eV) smaller VEEs.

Next, we investigate the lowest excitations for the diatomic species I_2 and TlH. For I_2, VEEs resulting from our calculations typically are slightly (ca. 0.1 eV) lower than those reported in ref 1 (Table 3 for both 1c and 2c treatments). This is also true for the 1c VEEs and might be the result of a different distance between the iodine atoms (1c BP86/QZVP optimized bond length in our calculation of 269.3 pm in ref 1, experimental bond length[78,82] of 266.6 pm) and the fact that we employ quadruple-ζ basis sets, whereas Wang et al. use basis sets of triple-ζ quality for their studies on diatomic molecules. Comparison with the few available experimental data yields a systematic underestimation for the LSDA VEEs belonging to the lowest five sublevels by about 0.4 eV. In contrast, the VEE for the transition to the 1_u sublevel of the energetically high-lying $^3\Sigma_u^+$ state is slightly overestimated by 0.1 eV. BP86 VEEs are usually somewhat smaller by up to 0.25 eV.

For TlH, our LSDA VEEs for both 1c and 2c treatments agree with those given in ref 1 within 0.02 eV (Table 4). Again, deviations may arise as we employ quadruple-ζ basis sets, whereas Wang et al. use basis sets of triple-ζ quality and the fact that the 1c BP86/QZVP optimized bond length in our calculation is 192.3 pm and the experimental bond length used in ref 1 is 187.0 pm.[78] This deviations in the VEEs are less than deviations resulting from exchanging the LSDA functional with BP86 (up to 0.1 eV) and less than differences to experimental data, which amount to up to 0.4 eV.

For all studied systems, exchanging QZVP by TZVP or QZVPP basis sets affects VEEs typically by 0.02 eV or less using LSDA (Tables I–IV, Supporting Information). The only exception is the transition to the $^1P_1$ state of Cd, where the TZVP VEE deviates from the QZVP or QZVPP VEE by slightly more than 0.2 eV for both the 2c and 1c value. This difference can be traced back to the lack of a diffuse *p* function in the TZVP basis set, which is present in the case of Hg. By adding a *p* function with an exponent of 0.02 to the TZVP basis set of Cd, the error for the transition to the $^1P_1$ state is reduced to less than 0.01 eV.

3.2. Demonstration of Efficiency: Electronic Spectrum of Au_{20}. Tedrahedral Au_{20} is an unusual cluster of metal atoms, as it comprises a comparably large gap between highest occupied MO (HOMO) and the lowest unoccupied MO (LUMO). Several calculations of VEEs for this system using different functionals are reported so far for 1c TDDFT methods. LDA or GGA functionals yield VEEs for the lowest transition with nonvanishing intensity of about 1.9 eV (for both ZORA and ECP approaches),[83,84] which is close to the HOMO−LUMO gap obtained with these functionals.[85] For hybrid functionals, a somewhat higher VEE for the lowest transition with nonvanishing intensity is obtained, e.g., this transition is found at 2.37 eV[86] using B3LYP,[87] and higher for

Table 3. Vertical Excitation Energies (VEEs) Using Scalar Relativistic (1c) TDDFT (states expressed in the Λ−Σ notation) as Well as Two-Component (2c) TDDFT (states expressed in the ω−ω notation) of I_2[a]

excited state	composition/contribution	degeneracy	BP86	LSDA	ref 1	exp.
scalar relativistic (1c)						
$^3\Pi_u$	0_u^+, 0_u^-, 1_u, 2_u	6	1.43	1.50	1.57	
$^1\Pi_u$	1_u	2	2.04	2.00	2.08	
$^3\Pi_g$	0_g^+, 0_g^-, 1_g, 2_g	6	2.98	3.07	3.20	
$^1\Pi_g$	1_g	2	3.58	3.56	3.71	
$^3\Sigma_u^+$	0_u^-, 1_u	3	4.29	4.55	4.69	
two-component (2c)						
2_u	$^3\Pi_u$	2	1.15	1.22	1.28	1.69[76]
1_u	$^3\Pi_u$	2	1.33	1.38	1.44	1.84[76]
0_u^-	$^3\Pi_u$	1	1.75	1.84	1.91	2.13[76]
0_u^+	$^3\Pi_u$	1	1.87	1.94	2.01	2.37[77]
1_u	$^1\Pi_u$	2	2.15	2.14	2.23	2.49[76]
2_g	$^3\Pi_g$	2	2.75	2.84	2.96	
1_g	$^3\Pi_g$	2	2.93	2.99	3.12	
0_g^-	$^3\Pi_g$	1	3.40	3.49	3.63	
0_g^+	$^3\Pi_g$	1	3.42	3.51	3.65	
1_g	$^1\Pi_g$	2	3.80	3.81	3.97	
0_u^-	$^3\Sigma_u^+$	1	4.43	4.69	4.83	
1_u	$^3\Sigma_u^+$	2	4.46	4.71	4.85	4.57[78]

[a]All calculated values were obtained using the BP86 and LSDA functional in combination with the dhf-QZVP-2c basis set and dhf-ecp-2c spin-orbit effective core potential (ECP). Degeneracies are also given. 2c VEEs obtained by Wang et al. are listed in column "ref 1". All values are in eV.

dx.doi.org/10.1021/ct400743r | J. Chem. Theory Comput. 2013, 9, 5341−5348

Table 4. Vertical Excitation Energies (VEEs) Using Scalar Relativistic (1c) TDDFT (states expressed in the Λ−Σ notation) as Well as Two-Component (2c) TDDFT (states expressed in the ω−ω notation) of TlH[a]

excited state	composition/contribution	degeneracy	BP86	LSDA	ref 1	exp.
scalar relativistic (1c)						
$^3\Pi$	0^+, 0^-, 1, 2	6	2.11	2.14	2.13	
$^1\Pi$	1	2	2.65	2.54	2.55	
two-component (2c)						
0^-	$^3\Pi$	1	1.83	1.89	1.88	
1	$^3\Pi$	2	2.02	2.05	2.05	
0^+	$^3\Pi$	1	2.03	2.09	2.08	2.20
1	$^1\Pi$	2	2.58	2.64	2.63	3.02
2	$^3\Pi$	2	2.90	2.86	2.88	3.00

[a] All calculated values were obtained using the BP86 and LSDA functional in combination with dhf-QZVP-2c basis sets and dhf-ecp-2c spin-orbit effective core potential (ECP) for Tl. Degeneracies are also given. All values are in eV. 2c VEEs obtained by Wang et al. are listed in column "ref 1". Experimental results are from ref 78.

long-range corrected functionals at 2.87 eV.[88] The latter are shown to more accurately describe the electronic excitation at least in Ag clusters,[89] and the same is believed to be true for Au clusters.

Nevertheless, although long-range corrected functionals might give more accurate results for the VEEs of Au_{20} than LDA and GGA functionals, we think it is worth studying the effect of SOC using the latter functionals, as some of the (triplet) excitations with zero OSs that are "spin-forbidden" in 1c treatments are expected to become "allowed" by SOC. Additionally, the whole spectrum might be shifted to lower energies because it is claimed that SOC reduces the HOMO−LUMO gap by about 0.37 eV.[90]

We calculated the lowest 57 VEEs within the 2c TDDFT formalism using LDA and GGA functionals in combination with QZVPP and TZVP basis sets and compared results and computational effort to 1c treatments. Main results of the 1c treatment at the BP86/QZVPP level are a HOMO−LUMO gap that can be considered the lowest VEE in zeroth order of 1.77 eV and the first VEE with nonvanishing OS ($1\ ^1T_2$) at 1.81 eV, in line with the previous studies mentioned above. All other calculated singlet excitations are "symmetry-forbidden", and all triplet excitations are "spin-forbidden" within the 1c theory.

Using 2c DFT we confirm that SOC reduces the HOMO−LUMO gap by 0.40 eV at the 2c BP86/QZVPP level. The entire spectrum at the 1c BP86/QZVPP level is shown in Figure 1, together with those resulting from the 2c treatments for variants BP86/QZVPP, BP86/TZVP, and LSDA/QZVPP. Respective numbers for VEEs including degeneracies as well as OSs (both in velocity and additionally in length representation) are given in Tables V−VI of the Supporting Information. Indeed, comparison of 1c and 2c BP86/QZVPP spectra shows that transitions with nonvanishing OS are observed for lower energies; three significant transitions (at about 1.60, 1.69, and 1.78 eV) are observed for the 2c case. As expected, including SOC in the calculation "allows" some of the transitions "forbidden" within a 1c theory. Using the smaller TZVP basis set leads to a systematic shift to higher energies by up to about 0.1 eV, whereas the corresponding OSs remain very similar. For the LSDA functional, we observe a shift of the first three significant transitions to smaller energies by up to about 0.1 eV.

We finally list the computational effort for the different treatments (always the lowest 57 excitations are calculated on a single Intel Xeon X5650 2.67 GHz processor, point group symmetry is not exploited in the calculations). The reference for the 1c treatment is an unrestricted determinant because this way both singlet and triplet excitations (without respective spin degeneracies) are included in the calculation simultaneously. At the 1c BP86/QZVPP level (number of basis functions N_{bf} = 2620), the computation time amounts to 42 h 30 min and at the respective 2c level it is 247 h 58 min. At the BP86/TZVP

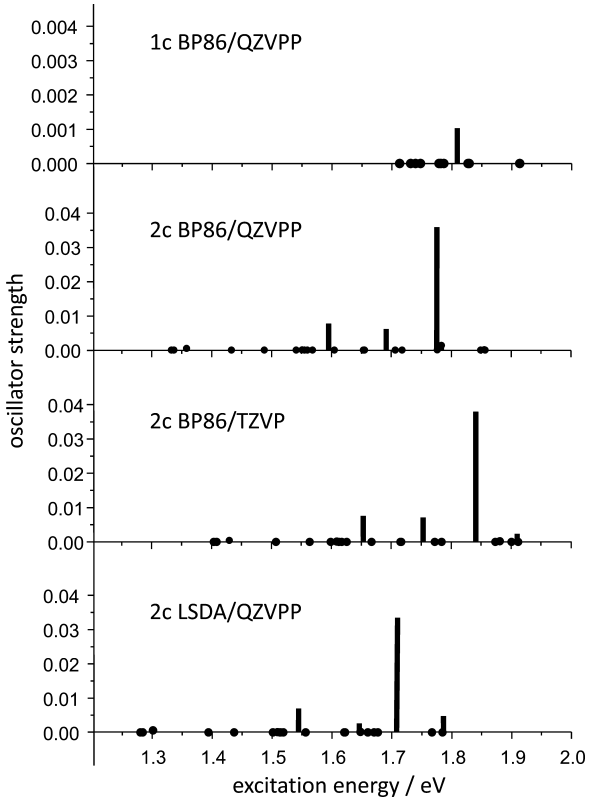

Figure 1. Electronic spectrum of Au_{20} (T_d symmetry). The oscillator strengths (OSs) in velocity representation are plotted against the vertical excitation energies (VEEs) in eV. The lowest 57 excitations are calculated (including degeneracies) using the following methods (from top to bottom): (a) Scalar relativistic (1c) TDDFT using dhf-QZVPP-2c basis sets and BP86 functional. (b) Two-component (2c) TDDFT using dhf-QZVPP-2c basis sets and BP86 functional. (c) Two-component (2c) TDDFT using dhf-TZVP-2c basis sets and BP86 functional. (d) Two-component (2c) TDDFT using dhf-QZVPP-2c basis sets and LSDA functional. dhf-ecp-2c spin−orbit effective core potential (ECP) is used. VEEs of excited states a marked with a dot if the corresponding OSs vanish in (a) or are close to zero in (b)-(d). Note the different scale of the vertical axis in (a).

level (N_{bf} = 1220), the times are 6 h 46 min (1c) and 38 h 31 min (2c). This reflects an increase of computational effort by $N_{bf}^{2.45}$ for the 2c procedure, which is almost the same as for the 1c treatment ($N_{bf}^{2.42}$). The speedup for the parallel version (4 processors) was estimated by calculation of the lowest 10 excitations at the BP86/TZVP level. It amounts to 2.8 for the 2c variant, similar to the 1c code (3.0).

4. CONCLUSIONS

We implemented a 2c TDDFT scheme for Kramers-restricted closed-shell systems using LDA and, to the best of our knowledge, for the first time, also GGA functionals with a proper GGA XC kernel. We mainly followed the route given by Wang et al.,[1] (noncollinear XC kernel) but used 2c ECPs instead of the all-electron ZORA approach and Gaussian-type instead of Slater-type basis functions. Our efficient code utilizes the RI approximation and accounts for solvent effects by COSMO. It also is parallelized following the scheme suggested by van Wüllen.[63] Differences in VEEs of selected atoms, ions, and diatomic molecules to results obtained in ref 1 with LDA functionals are smaller than deviations resulting from exchanging LDA by GGA functionals and are by far smaller than differences to experimental values. Routine applications are possible on a single processor for systems of several thousand basis functions, as demonstrated by calculation of the lowest 57 excitations of Au_{20} with a basis set of quadruple-ζ valence quality, which took about 248 h and yielded nonzero OSs for several "spin-forbidden" transitions below the first "spin-allowed" transition. The parallel version yields reasonable speedups, e.g., 2.8, when using four processors, which is similar as for 1c treatments of the same system.

■ ASSOCIATED CONTENT

Supporting Information

Detailed description of the implemented 2c TDDFT algorithm. Tables of 1c and 2c VEEs of all investigated atoms, ions, and diatomic molecules calculated using different basis sets in combination with the LSDA functional. 1c and 2c VEEs including degeneracies and OSs (in velocity and length representations) of Au_{20} calculated using different basis sets and density functionals. Coordinates of all structures. This material is available free of charge via the Internet at http://pubs.acs.org.

■ AUTHOR INFORMATION

Corresponding Author

*E-mail: florian.weigend@kit.edu.

Notes

The authors declare no competing financial interest.

■ ACKNOWLEDGMENTS

The authors thank F. Furche for helpful discussions. M.K. is funded by the Carl Zeiss Foundation and also thanks TURBOMOLE GmbH for financial support.

■ REFERENCES

(1) Wang, F.; Ziegler, T.; van Lenthe, E.; van Gisbergen, S.; Baerends, E. J. *J. Chem. Phys.* **2005**, *122*, 204103.
(2) *Time-Dependent Density Functional Theory*; Marques, M. A. L., Ullrich, C. A., Nogueira, F., Rubio, A., Burke, K., Gross, E. K. U., Eds.; Lecture Notes in Physics; Springer, Heidelberg, 2006.
(3) Furche, F. *J. Chem. Phys.* **2001**, *114*, 5982−5992.
(4) Rosa, A.; Baerends, E. J.; van Gisbergen, S. J. A.; van Lenthe, E.; Groeneveld, J. A.; Snijders, J. G. *J. Am. Chem. Soc.* **1999**, *121*, 10356−10365.
(5) van Lenthe, E.; Baerends, E. J.; Snijders, J. G. *J. Chem. Phys.* **1993**, *99*, 4597−4610.
(6) van Lenthe, E.; Baerends, E. J.; Snijders, J. G. *J. Chem. Phys.* **1994**, *101*, 9783−9792.
(7) van Lenthe, E.; Ehlers, A. W.; Baerends, E. J. *J. Chem. Phys.* **1999**, *110*, 8943−8953.
(8) Andrae, D.; Häußermann, U.; Dolg, M.; Stoll, H.; Preuß, H. *Theor. Chim. Acta* **1990**, *77*, 123−141.
(9) Bergner, A.; Dolg, M.; Küchle, W.; Stoll, H.; Preuß, H. *Mol. Phys.* **1993**, *80*, 1431−1441.
(10) Küchle, W.; Dolg, M.; Stoll, H.; Preuß, H. *Mol. Phys.* **1991**, *74*, 1245−1263.
(11) Leiniger, T.; Nicklass, A.; Küchle, W.; Stoll, H.; Dolg, M.; Bergner, A. *Chem. Phys. Lett.* **1996**, *255*, 274−280.
(12) Kaupp, M.; Schleyer, P. V.; Stoll, H.; Preuß, H. *J. Chem. Phys.* **1991**, *94*, 1360−1366.
(13) Rajagopal, A. K. *Phys. Rev. A* **1994**, *50*, 3759−3765.
(14) Gao, J.; Liu, W.; Song, B.; Liu, C. *J. Chem. Phys.* **2004**, *121*, 6658−6666.
(15) Gao, J.; Zou, W.; Liu, W.; Xiao, Y.; Peng, D.; Song, B.; Liu, C. *J. Chem. Phys.* **2005**, *123*, 054102.
(16) Bast, R.; Jensen, H. J. A.; Saue, T. *Int. J. Quantum Chem.* **2009**, *109*, 2091−2112.
(17) Peng, D.; Zou, W.; Liu, W. *J. Chem. Phys.* **2005**, *123*, 144101.
(18) Amsterdam Density Functional (ADF), version 2013.01a. http://www.scm.com.
(19) Liu, W.; Hong, G.; Dai, D.; Li, L.; Dolg, M. *Theor. Chem. Acc.* **1997**, *96*, 75−83.
(20) Liu, W.; Wang, F.; Li, L. *J. Theor. Comput. Chem.* **2003**, *2*, 257−266.
(21) Liu,W.;Wang, F.; Li, L. *Recent Advances in Relativistic Molecular Theory*; World Scientific, Singapore, 2004; Vol. *5*, p 257.
(22) Aa, H. J.; Jensen, R.; Bast, T. S.; Visscher, L.; Bakken, V.; Dyall, K. G.; Dubillard, S.; Ekström, U.; Eliav, E.; Enevoldsen, T.; Fleig, T.; Fossgaard, O.; Gomes, A. S. P.; Helgaker, T.; Lærdahl, J. K.; Lee, Y. S.; Henriksson, J.; Iliaš, M.; Jacob, Ch. R.; Knecht, S.; Komorovský, S.; Kullie, O.; Larsen, C. V.; Nataraj, H. S.; Norman, P.; Olejniczak, G.; Olsen, J.; Park, Y. C.; Pedersen, J. K.; Pernpointner, M.; Ruud, K.; Sałek, P.; Schimmelpfennig, B.; Sikkema, J.; Thorvaldsen, A. J.; Thyssen, J.; van Stralen, J.; Villaume, S.; Visser, O.; Winther, T.; Yamamoto, S. DIRAC, a Relativistic ab Initio Electronic Structure Program, Release DIRAC12, 2012. http://www.diracprogram.org.
(23) Iliaš, M.; Saue, T. *J. Chem. Phys.* **2007**, *126*, 064102.
(24) van Wüllen, C. *J. Comput. Chem.* **2002**, *23*, 779−785.
(25) Wang, F.; Liu, W. *J. Chin. Chem. Soc. (Taipei)* **2003**, *50*, 597−606.
(26) Mayer, M.; Häberlen, O. D.; Rösch, N. *Phys. Rev. A* **1996**, *54*, 4775−4782.
(27) Liu, W.; van Wüllen, C. *J. Chem. Phys.* **1999**, *110*, 3730−3735.
(28) Liu, W.; van Wüllen, C.; Han, Y.-K.; Choi, Y.-J.; Lee, Y.-S. *Adv. Quantum Chem.* **2001**, *39*, 325−355.
(29) Wang, F.; Ziegler, T. *J. Chem. Phys.* **2005**, *123*, 194102.
(30) Liao, Y.; Yang, G.-C.; Feng, J.-K.; Shi, L.-L.; Yang, S.-Y.; Yang, L.; Ren, A.-M. *J. Phys. Chem. A* **2006**, *110*, 13036−13044.
(31) Shi, L.-L.; Liao, Y.; Zhao, L.; Su, Z.-M.; Kan, Y.-H.; Yang, G.-C.; Yang, S.-Y. *J. Organomet. Chem.* **2007**, *692*, 5368−5374.
(32) Ramirez-Tagle, R.; Arratia-Pérez, R. *Chem. Phys. Lett.* **2008**, *460*, 438−441.
(33) Muñoz-Castro, A.; Carey, D. M.-L.; Arratia-Pérez, R. *Chem. Phys. Lett.* **2009**, *474*, 290−293.
(34) Zhu, Y.-L.; Zhou, S.-Y.; Kan, Y.-H.; Su, Z.-M. J. *Organomet. Chem.* **2009**, *694*, 3012−3018.
(35) Shi, L.-L.; Geng, Y.; Gao, H.-Z.; Su, Z.-M.; Wu, Z.-J. *Dalton Trans.* **2010**, *39*, 7733−7740.

(36) Baranoff, E.; Curchod, B. F. E.; Frey, J.; Scopelliti, R.; Kessler, F.; Tavernelli, I.; Rothlisberger, U.; Grätzel, M.; Nazeeruddin, M. K. *Inorg. Chem.* **2012**, *51*, 215−224.
(37) Baranoff, E.; Curchod, B. F. E.; Monti, F.; Steimer, F.; Accorsi, G.; Tavernelli, I.; Rothlisberger, U.; Scopelliti, R.; Grätzel, M.; Nazeeruddin, M. K. *Inorg. Chem.* **2012**, *51*, 799−811.
(38) Heydová, R.; Gindensperger, E.; Romano, R.; Sýkora, J.; Vlček, A., Jr.; Záliš, S.; Daniel, C. *J. Phys. Chem. A* **2012**, *116*, 11319−11392.
(39) Casarin, M.; Finetti, P.; Vittadini, A.; Wang, F.; Ziegler, T. *J. Phys. Chem. A* **2007**, *111*, 5270−5279.
(40) Stener, M.; Nardelli, A.; Fronzoni, G. *Chem. Phys. Lett.* **2008**, *462*, 358−364.
(41) Tecmer, P.; Bast, R.; Ruud, K.; Visscher, L. *J. Phys. Chem. A* **2012**, *116*, 7397−7404.
(42) Armbruster, M. K.; Weigend, F.; van Wüllen, C.; Klopper, W. *Phys. Chem. Chem. Phys.* **2008**, *10*, 1748−1756.
(43) Local version of TURBOMOLE V6.5 2013, a development of University of Karlsruhe and Forschungszentrum Karlsruhe GmbH, 1989−2007, TURBOMOLE GmbH since 2007.
(44) Peterson, K. A.; Figgen, D.; Dolg, M.; Stoll, H. *J. Chem. Phys.* **2007**, *126*, 124101.
(45) Figgen, D.; Peterson, K. A.; Dolg, M.; Stoll, H. *J. Chem. Phys.* **2009**, *130*, 164108.
(46) Figgen, D.; Rauhut, G.; Dolg, M.; Stoll, H. *Chem. Phys.* **2005**, *311*, 227−244.
(47) Metz, B.; Stoll, H.; Dolg, M. *J. Chem. Phys.* **2000**, *113*, 2563−2569.
(48) Peterson, K. A.; Figgen, D.; Goll, E.; Stoll, H.; Dolg, M. *J. Chem. Phys.* **2003**, *119*, 11113−11123.
(49) Lim, I. S.; Schwerdtfeger, P.; Metz, B.; Stoll, H. *J. Chem. Phys.* **2005**, *122*, 104103.
(50) Lim, I. S.; Stoll, H.; Schwerdtfeger, P. *J. Chem. Phys.* **2006**, *124*, 034107.
(51) Bauernschmitt, R.; Ahlrichs, R. *Chem. Phys. Lett.* **1996**, *256*, 454−464.
(52) Wang, F.; Ziegler, T. *J. Chem. Phys.* **2004**, *121*, 12191−12196.
(53) Wang, F.; Ziegler, T. *Int. J. Quantum Chem.* **2006**, *106*, 2545−2550.
(54) Rinkevicius, Z.; Vahtras, O.; Ågren, H. *J. Chem. Phys.* **2010**, *133*, 114104.
(55) Kühn, M.; Weigend, F. *Chem. Phys. Chem.* **2011**, *12*, 3331−3336.
(56) Li, Z.; Liu, W. *J. Chem. Phys.* **2012**, *136*, 024107.
(57) Bernard, Y. A.; Shao, Y.; Krylov, A. I. *J. Chem. Phys.* **2012**, *136*, 204103.
(58) Furche, F.; Rappoport, D. *Computational Photochemistry*; Elsevier, Amsterdam, 2005; Vol. *16*, p 93.
(59) Bauernschmitt, R.; Häser, M.; Treutler, O.; Ahlrichs, R. *Chem. Phys. Lett.* **1997**, *264*, 573−578.
(60) Davidson, E. R. *J. Comput. Phys.* **1975**, *17*, 87−94.
(61) Olsen, J.; Jensen, H. J. A.; Jørgensen, P. *J. Comput. Phys.* **1988**, *74*, 265−282.
(62) Eichkorn, K.; Weigend, F.; Treutler, O.; Ahlrichs, R. *Theor. Chem. Acc.* **1997**, *97*, 119−124.
(63) van Wüllen, C. *J. Comput. Chem.* **2010**, *32*, 1195−1201.
(64) Klamt, A. *J. Phys. Chem.* **1996**, *100*, 3349−3353.
(65) Scalmani, G.; Frisch, M. J.; Mennucci, B.; Tomasi, J.; Cammi, R.; Barone, V. *J. Chem. Phys.* **2006**, *124*, 094107.
(66) Becke, A. D. *Phys. Rev. A* **1988**, *38*, 3098−3100.
(67) Perdew, J. P. *Phys. Rev. B* **1986**, *33*, 8822−8824.
(68) Weigend, F.; Baldes, A. *J. Chem. Phys.* **2010**, *133*, 174102.
(69) Tao, J.; Perdew, J. P.; Staroverov, V. N.; Scuseria, G. E. *Phys. Rev. Lett.* **2003**, *91*, 146401.
(70) Perdew, J. P.; Wang, Y. *Phys. Rev. B* **1992**, *45*, 13244−13249.
(71) Rappoport, D.; Furche, F. *J. Chem. Phys.* **2010**, *133*, 134105.
(72) Weigend, F. *Phys. Chem. Chem. Phys.* **2006**, *8*, 1057−1065.
(73) Armbruster, M. K.; Klopper, W.; Weigend, F. *Phys. Chem. Chem. Phys.* **2006**, *8*, 4862−4865.
(74) Treutler, O.; Ahlrichs, R. *J. Chem. Phys.* **1995**, *102*, 346−354.
(75) Moore, C. E. *Atomic Energy Levels*, Vols. *1*−3; Circular No. 467; National Bureau of Standards: Washington, DC , 1949, 1952, 1958.
(76) Tellinghuisen, J. *J. Chem. Phys.* **1973**, *58*, 2821−2824.
(77) Tellinghuisen, J. *J. Chem. Phys.* **1982**, *76*, 4736−4744.
(78) Huber, K. P.; Herzberg, G. *Molecular Spectra and Molecular Structure*, Vol. *IV*; Van Nostrand and Reinhold, New York, 1979.
(79) Dirac, P. A. M. *Proc. R. Soc. London, Ser. A* **1929**, *123*, 714−733.
(80) Slater, J. C. *Phys. Rev.* **1951**, *81*, 385−390.
(81) Vosko, S. H.; Wilk, L.; Nusair, M. *Can. J. Phys.* **1980**, *58*, 1200−1211.
(82) Howard, W. F., Jr.; Andrews, L. *J. Raman Spectrosc.* **1974**, *2*, 447−462.
(83) Idrobo, J. C.; Walkosz, W.; Yip, S. F.; Öğüt, S.; Wang, J.; Jellinek, J. *Phys. Rev. B* **2007**, *76*, 205422.
(84) Aikens, C. M.; Schatz, G. C. *J. Phys. Chem. A* **2006**, *110*, 13317−13324.
(85) Kryachko, E. S.; Remacle, F. *Int. J. Quantum Chem.* **2007**, *107*, 2922−2934.
(86) Xie, R.-H.; Bryant, G. W.; Zhao, J.; Kar, T.; Smith, V. H., Jr. *Phys. Rev. B* **2005**, *71*, 125422.
(87) Becke, A. D. *J. Chem. Phys.* **1993**, *98*, 5648−5652.
(88) Koppen, J. V.; Hapka, M.; Szczęśniak, M. M.; Chałasínski, G. *J. Chem. Phys.* **2012**, *137*, 114302.
(89) Silverstein, D. W.; Jensen, L. *J. Chem. Phys.* **2010**, *132*, 194302.
(90) Li, J.; Li, X.; Zhai, H.-J.; Wang, L.-S. *Science* **2003**, *299*, 864−867.